Available online at www.sciencedirect.com
ScienceDirect
European Journal of Pharmaceutics and Biopharmaceutics 68 (2008) 676–687
European Journal of Pharmaceutics and Biopharmaceutics
www.elsevier.com/locate/ejpb

Research paper

Cell line-dependent internalization pathways and intracellular trafficking determine transfection efficiency of nanoparticle vectors

Kimberly L. Douglas [a], Ciriaco A. Piccirillo [b,*], Maryam Tabrizian [a,c,*]

[a] Department of Biomedical Engineering, McGill University, Montreal, Que., Canada
[b] Department of Microbiology and Immunology, McGill University, Montreal, Que., Canada
[c] Centre for Biorecognition and Biosensors, McGill University, Montreal, Que., Canada

Received 6 June 2007; accepted in revised form 7 September 2007
Available online 15 September 2007

Abstract

It has been suggested that cell physiology may affect the internalization pathways of non-viral vectors, leading to cell line-dependent transfection efficiency. To verify this hypothesis, fluorescently labeled alginate–chitosan nanoparticle complexes were used as non-viral vectors to transfect 293T, COS7, and CHO cells and to observe the cellular interactions and internalization mechanisms of the complexes in each cell line. 293T cells, which demonstrate the highest transfection efficiency, internalize complexes primarily through clathrin-mediated processes. COS7 cells also demonstrate some internalization of complexes through the clathrin-dependent pathway, explaining the moderate transfection exhibited. In contrast, CHO cells internalize complexes predominantly through caveolin-mediated pathways and are not transfected. Results suggest that following clathrin-mediated endocytosis, complexes are trafficked to the endo-lysosomal pathway, where the proton-sponge effect leads to their release into the cytosol. Contrarily, the absence of trafficking to this pathway following caveolin-mediated endocytosis results in vesicle-entrapped complexes that become transfection-incompetent. These results demonstrate that cell physiology is a critical factor in efficient transfection, and that trafficking to the endo-lysosomal pathway through specific internalization mechanisms is essential for transfection with alginate–chitosan nanoparticle complexes.
© 2007 Elsevier B.V. All rights reserved.

Keywords: Non-viral vector; Internalization; Transfection; Intracellular trafficking; Caveolin; Clathrin

1. Introduction

The frequency of reports on the development of new non-viral vectors suggests that gene delivery to cells in a safe and efficient manner remains an elusive goal. Cationic lipids and polymers have been used extensively in the production of non-viral vectors due to their ability to associate with DNA through charge interactions to form compact complexes, which facilitates cellular entry and protects DNA from nuclease attack and degradation [1]. Although non-viral vectors lead to significant improvements in cellular penetration, protection, and transfection over naked DNA, they have not yet achieved consistent transfection suitable for practical applications [2].

The inability to explain or predict transfection efficiencies may result from the general lack of consideration as to how internalization mechanisms impact transfection. Non-viral vectors are evaluated predominantly through gene expression, a method that evaluates transfection but provides no insight into the capacity of complexes to evade specific barriers [3]. The following processes represent the greatest obstacles to vector-mediated transfection: internalization, avoidance of lysosomal degradation, escape to the cytoplasm, and trafficking to the nucleus.

* Corresponding authors. Faculty of Dentistry, Centre for Biorecognition and Biosensors, McGill University, 3775 University Street, Montreal, Que., Canada H3A 2B4 (M. Tabrizian). Tel.: +514 398 8129; fax: +514 398 7461; Department of Biomedical Engineering, McGill University, 3775 University Street, Montreal, Que., Canada H3A 2B4 (C.A. Piccirillo).
E-mail addresses: maryam.tabrizian@mcgill.ca (M. Tabrizian), ciriaco.piccirillo@mcgill.ca (C.A. Piccirillo).

0939-6411/$ - see front matter © 2007 Elsevier B.V. All rights reserved.
doi:10.1016/j.ejpb.2007.09.002

As the first step in effective transfection, elucidating the mechanism of vector uptake is a prerequisite to understanding and improving transfection. It is generally accepted that non-viral vectors enter cells via endocytosis, of which mammalian cells demonstrate a number of distinct processes. Some of these processes include clathrin- and caveolin-mediated endocytosis, macropinocytosis, and phagocytosis, as well as via cholesterol-mediated lipid rafts [4–6]. Recent studies have failed to demonstrate the dominance of any particular uptake pathway leading to transfection. Further confounding this issue are the effects of size, charge, nature, and stability of the complexes on their cellular internalization and trafficking [7–12]. These factors make it evident that greater consideration of the uptake and trafficking mechanisms is required to design vectors that maximize transfection.

We recently reported the application of newly developed alginate–chitosan nanoparticles as a gene delivery system [13]. To improve upon the efficiency of chitosan nanoparticles while maintaining non-toxicity, biocompatibility, and biodegradability, alginate–chitosan nanoparticles were prepared through spontaneous complex coacervation forming particles with a mean size of 157 nm and a zeta potential of +32 mV. Nanoparticles mediated transfection of 293T cells four times that achieved by chitosan nanoparticles, with the increased transfection attributed to reduced strength of interaction between chitosan and DNA due to the presence of alginate.

Since cell line-dependent transfection has been reported for numerous vectors [14–19], the purpose of this study was to examine the transfection efficiency of alginate–chitosan nanoparticles in multiple cell lines and to correlate this to the internalization mechanisms and intracellular trafficking of the vectors. The three cell lines used in this study, 293T, COS7, and CHO cells, were chosen to represent different cell types, distinct mammals, and organs.

2. Materials and methods

2.1. Cell cultures

Three cell lines were used in this study: 293T, COS7, and CHO. CHO cells were grown in Alpha Minimum Essential Medium (αMEM), while 293T and COS7 cells were cultured in Dulbecco's Modified Eagle's Medium (DMEM). Medium was supplemented with 10% (v/v) fetal bovine serum (FBS, ATCC, USA) and 1% penicillin/streptomycin. Cells were cultured at 37 °C in a humidified 5% CO_2 atmosphere and sub-cultured prior to confluence using trypsin–EDTA. Cell culture media, penicillin/streptomycin and trypsin–EDTA were obtained from Gibco (Burlington, Ont., Canada).

2.2. Plasmid DNA

Two plasmids, pEGFP-N1 (Clontech, USA) encoding for green fluorescent protein, and pCMV-Luc (a generous gift from M. Olivier, McGill University) encoding for firefly luciferase, were used to prepare nanoparticle–DNA complexes and to monitor gene transfer and transgene expression after transfection. Plasmids were amplified and isolated using a Plasmid Maxi Kit (QIAGEN, Mississauga, Ont., Canada) or PureLink HiPure Plasmid Maxiprep Kit (Invitrogen, Burlington, Ont., Canada). Plasmid concentration was measured by UV absorption at 260 nm and purity was determined using agarose gel electrophoresis.

2.3. Complex preparation

Alginate–chitosan nanoparticles were prepared as previously described [13]. Briefly, nanoparticles were prepared by mixing 0.005% (w/v) sodium alginate (Sigma, Oakville, Ont., Canada) and 1% (w/v) chitosan (Carbomer, San Diego, CA, USA), each dissolved in MilliQ water and pH adjusted to 5.6–5.9 using 1 M HCl, to give a final weight ratio of 1:1.5 alginate:chitosan and stirred for 1 h at room temperature. Labeled nanoparticles, prepared using fluorescein-labeled chitosan (Carbomer, San Diego, CA, USA), were used for confocal microscopy and internalization studies. Non-labeled nanoparticles were used for transfection assays. Complexes were prepared by adding DNA to the nanoparticle suspension to give the desired N:P ratio and incubated at room temperature for 30 min prior to use. (N:P ratio is the ratio of the available amino groups in the alginate–chitosan nanoparticles to the DNA phosphate groups.)

2.4. Cell viability

293T, COS7, and CHO cells were seeded in 48-well plates at densities of 4×10^4, 1.5×10^4, and 2×10^4 cells/well, respectively, in phenol red-free medium supplemented with 10% (v/v) FBS. The following day, the medium was removed and replaced with 200 μL medium containing 40, 80, or 125 μg/mL alginate–chitosan nanoparticles complexed with 1 μg DNA (equivalent amounts to those used in other assays, with N:P ratios of 2:1, 3.7:1, and 5.6:1, respectively). Lipofectamine™ (5 μg/mL, Invitrogen) complexed with 1 μg DNA was used as a control. Cells were incubated for 24 h, after which time the MTT assay was performed according to directions (Vybrant MTT Assay, Molecular Probes). Briefly, the treatment medium was replaced with 300 μL culture medium to which 30 μL MTT (12 mM in PBS) was added. After 4 h incubation at 37 °C, 300 μL SDS–HCl was added followed by a further incubation at 37 °C (4 h). Sample absorbance at 570 nm was then measured by a plate spectrophotometer (μQuant, Bio-Tek Instruments Inc.). The viability of cells incubated with culture medium alone was set as 100%.

2.5. In vitro transfection

In 24-well plates 293T, COS7, and CHO cells were seeded at 5×10^4, 3×10^4, and 4×10^4 cells/well, respec-

tively, the day prior to transfection. For transfection, the culture medium was replaced with 300 μL serum-free medium containing unlabeled nanoparticle–DNA complexes of N:P charge ratios of 1:2, 1:1, 2:1, and 5:1, with each well receiving 2 μg pEGFP-N1. As a positive control, cells were treated with 4 μL Lipofectamine™ (Invitrogen, Mississauga, Ont., Canada) complexed with 2 μg DNA. As a negative control, cells were treated with unlabeled alginate–chitosan nanoparticles, containing no DNA. After 4 h, the medium was increased to 500 μL with medium supplemented with 10% (v/v) FBS; the medium was replaced with fresh complete medium (containing FBS and penicillin/streptomycin) after 24 h. Transfection was assessed 48 h post-transfection using flow cytometry. Cells were removed using cold EDTA (0.6 mM in PBS), transferred to tubes, washed with PBS, and analyzed directly (FACSCalibur). Ten thousand events were measured in each sample.

2.6. Confocal microscopy

Following results of the transfection assay, additional studies were undertaken to examine the intracellular uptake and trafficking of the complexes. Studies to optimize complex parameters for uptake revealed that the dose and N:P ratio of complexes affected binding and uptake in all three cell lines, with increased uptake resulting from increasing doses and increasing N:P ratios. The highest fraction of cell-associated fluorescence resulted from N:P ratios between 3:1 and 6:1 (data not shown). Based on these results, uptake experiments were performed with complexes prepared at N:P ratios of 3.7:1 for CHO and COS7 cells, and of 5.6:1 for 293T cells. For all uptake studies, complexes of fluorescein-labeled nanoparticles and pEGFP-N1 were used.

Cells were seeded 24 h prior to treatment in 12-well plates containing glass cover slips at 1×10^5 (293T), 6×10^4 (COS7), and 8×10^4 (CHO) cells/well in medium containing 10% (v/v) FBS. For treatment, the medium was removed and cells were washed once with phosphate buffer solution (PBS, Sigma, Oakville, Ont., Canada) prior to the addition of 600 μL of the treatment solution, which consisted of LysoTracker Red™ (75 nM) (Molecular Probes, Eugene, OR, USA) in serum-free medium with complexes containing 4 μg of pEGFP-N1. At specified intervals (30 min, 1 h, 2 h, and 4 h), the treatment medium was removed, cells were washed twice in cold PBS, and fixed with paraformaldehyde (4%, 20 min) (Sigma, Oakville, Ont., Canada). Cover slips were washed twice with PBS, then incubated with DAPI (300 nM 4′,6-diamidino-2-phenylindole dihydrochloride in PBS) (Molecular Probes, Eugene, OR, USA) for 3 min to stain nuclei. Following two additional washes with PBS, cover slips were mounted on slides using GelTol mounting medium (Thermo Electron Corporation, Waltham, MA, USA). Slides were analyzed using a confocal microscope (LSM510 META, Carl Zeiss, Germany) with the following excitation and emission wavelengths: fluorescein excitation 488 nm, emission band pass 505–530 nm; DAPI excitation 405 nm, emission band pass 420–480 nm; LysoTracker Red excitation 543 nm, emission band pass 560–615 nm. Slides of untreated cells were used as a negative control to determine microscope settings, which were maintained for all image capture and analysis. Images were obtained of three randomly selected areas of two separate slides for each treatment. All areas were analyzed using *Z*-sectioning.

2.7. Flow cytometry analysis

One day prior to treatment with nanoparticle complexes 293T, COS7, and CHO cells were seeded in 24-well plates at 8×10^4, 3×10^4, and 4×10^4 cells/well, respectively. For treatment, the medium was removed and cells were washed once with PBS prior to addition of 300 μL of treatment solution, containing 2 μg of pEGFP-N1 within the fluorescein-labeled complexes. At specified intervals (0 min, 15 min, 30 min, 1 h, 2 h, and 4 h), the medium was removed and the cells were washed with cold PBS. (Note that for the 0 min treatment, medium containing complexes was added to wells, the well was rocked once, and the medium was subsequently removed. Total exposure time was less than 1 min.) Except where noted, cells were treated with trypan blue (0.04% in PBS) for 1 min to quench external fluorescence and washed again with PBS before being detached using cold EDTA (0.6 mM in PBS) [4]. In all cases, cells were removed to tubes, centrifuged and resuspended in PBS, and analyzed directly (FACSCalibur, BD Biosciences, Mississauga, Ont., Canada). Five to ten thousand events were measured for each sample; appropriate controls and gates were used for analysis.

The uptake study was repeated under various conditions designed to directly affect binding and to ascertain trafficking to lysosomes. Treatment in the presence of excess chitosan, equivalent to the amount in the nanoparticle complexes (0.05 μg/μL), was done to detect saturable or receptor-mediated processes. In one set of experiments, cells were detached using trypsin–EDTA to remove nanoparticles associated with surface proteins. With these two treatments (excess chitosan and trypsinization), trypan blue quenching was not performed. In a separate set of experiments, cells were incubated with monensin (25 μM in PBS) (Sigma, Oakville, Ont., Canada) following detachment for 30 min at 4 °C to neutralize late endosomal and lysosomal pH and thereby reverse quenching of fluorescein fluorescence, which is inhibited at acidic pH. To promote endosomal escape, cells were treated with complexes in the presence of chloroquine (100 μM) (Sigma, Oakville, Ont., Canada), with no pre-treatment.

2.8. Uptake inhibition

The identification of specific endocytic processes involved in complex internalization was done through uptake assays in the presence of chemicals known to inhibit certain pathways. In all cases, optimization studies were

performed to maximize the effects of the chemicals while minimizing their inherent toxicity. Cytoskeleton reorganization was prevented by incubating the cells with cytochalasin D (10 μg/mL) (Sigma, Oakville, Ont., Canada) for 30 min followed by application of nanoparticle complexes. Macropinocytosis was promoted through treatment with phorbol myristate acetate (PMA, 1 μM) (Sigma, Oakville, Ont., Canada) for 30 min prior to addition of the complexes. Clathrin-dependent endocytosis was disturbed by co-treatment with chlorpromazine (10 μg/mL) (Sigma, Oakville, Ont., Canada), following a 30 min pre-incubation at the same concentration. To perturb caveolin-mediated pathways, cells were pre-treated with genistein (200 μg/mL) (Sigma, Oakville, Ont., Canada) for 30 min. In all cases, treatment of the cells with nanoparticle–DNA complexes was done in the presence of the respective drug at the same concentration as used for the pre-treatment. Following treatment under these various conditions, cells were harvested at specific intervals (15 min, 30 min, 1 h, 2 h, and 4 h), prepared and analyzed as described above.

2.9. Uptake inhibition and in vitro transfection

Following results of uptake inhibition assays, transfection of 293T and COS7 cells was repeated in the presence of chlorpromazine or genistein to determine the effect of uptake inhibitors on transfection. (Since transfection was not successful in CHO cells, the assay was not performed with that cell line.) In 24-well plates 293T and COS7 cells were seeded at 5×10^4 and 3×10^4 cells/well, respectively, the day prior to transfection. Thirty minutes prior to transfection cells were treated with either chlorpromazine or genistein, as described above. For transfection, the culture medium was replaced with 300 μL serum-free medium containing either chlorpromazine or genistein and unlabeled nanoparticle–DNA complexes with each well receiving 2 μg pCMV-Luc. As a positive control, cells were treated with 4 μL Lipofectamine™ (Invitrogen, Mississauga, Ont., Canada) complexed with 2 μg DNA. As a negative control, cells were treated with unlabeled alginate–chitosan nanoparticles, containing no DNA. After 4 h, the medium was increased to 500 μL with medium supplemented with 10% (v/v) FBS; the medium was replaced with fresh complete medium (containing FBS and penicillin/streptomycin) after 24 h.

Cells were analyzed after 48 h. Cells were removed using cold EDTA (0.6 mM in PBS), transferred to micro-centrifuge tubes, and resuspended in cell culture lysis reagent (Luciferase Assay Kit, Promega BioSciences, Madison, WI, USA). Following centrifugation at 12,000*g* for 1 min, 20 μL aliquots of the supernatant were removed, added to 100 μL luciferase assay reagent, and analyzed using a luminometer (MiniLumat LB 9506, Berthold Technologies, Germany) over 30 s. Appropriate controls were used for analysis. Results are reported as relative light units per mg of protein, with protein content determined using a standard BCA assay (Pierce Biotechnology, Rockford, IL, USA).

2.10. Statistical analysis

All experiments were repeated three times and analyzed in triplicate. Results reported are means and standard deviations, unless otherwise noted. Statistical significance was determined using Student's two-sided *t*-test with $P < 0.05$ deemed significant.

3. Results

3.1. Effect of alginate–chitosan nanoparticle complexes on cell viability

Cells were incubated with alginate–chitosan nanoparticle–DNA complexes for 24 h, after which time the MTT assay was used to assess cell viability. Complexes show no toxicity to any of the cell lines when incubated at low N:P ratios (Fig. 1). Alginate–chitosan complexes are significantly less toxic than Lipofectamine™ in all cell lines and at all ratios, with the exception of 293T cells exposed to the highest concentration of alginate–chitosan nanoparticle complexes.

3.2. Cell line-dependent transfection

Cells were transfected with the pEGFP-N1 plasmid coding for the green fluorescent protein and analyzed using flow cytometry after 48 h. Results, expressed as percentage of cells transfected or change in mean fluorescence intensity, demonstrated a clear dependence of transfection efficiency on the cell line, as well as on the charge ratio of the alginate–chitosan nanoparticle complexes (Fig. 2).

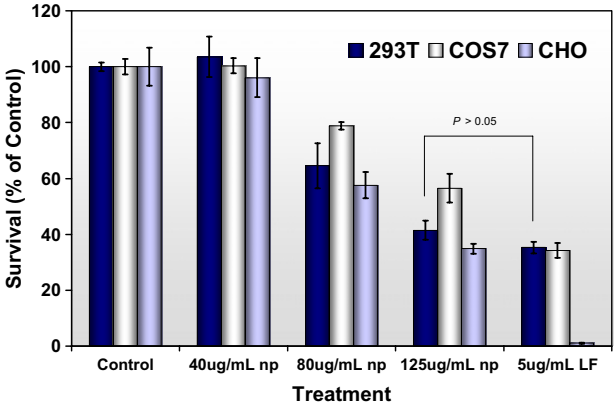

Fig. 1. Results of MTT assay demonstrating biocompatibility of alginate–chitosan complexes (np) compared to Lipofectamine™ (LF). COS7 cells demonstrate a reduced sensitivity to the complexes as demonstrated by increased survival compared to both 293T and CHO cells at higher concentrations of complexes. Alginate–chitosan complexes at the lowest concentration had no effect on cell viability. Treatment with either alginate–chitosan complexes at higher concentrations or with Lipofectamine™ reduced survival significantly compared to controls ($P < 0.05$). Alginate–chitosan complexes were significantly less cytotoxic than Lipofectamine™ at all concentrations and for all cell lines, with the exception of 293T cells treated at the highest concentration of complexes. Values represent the means ± standard deviation ($n = 3$).

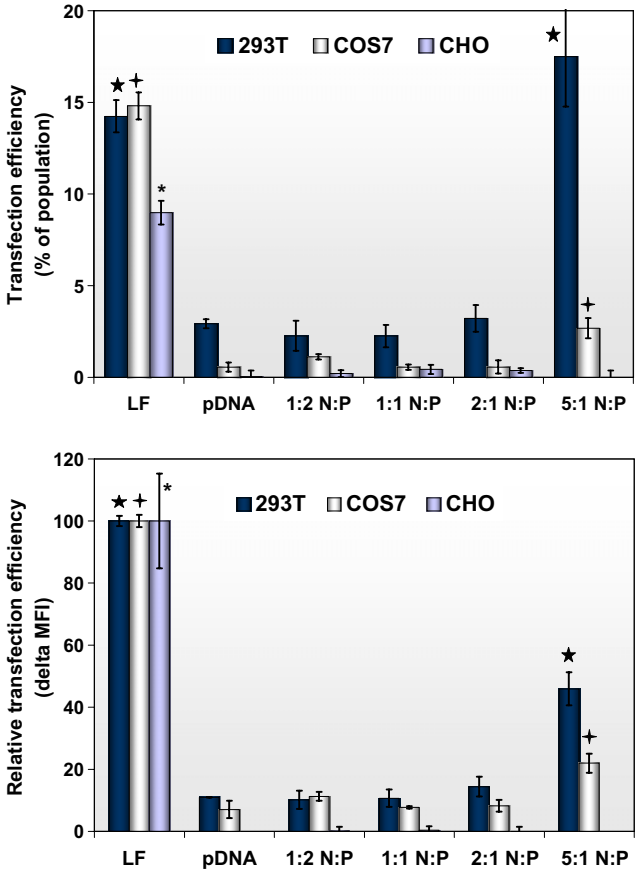

Fig. 2. Transfection efficiency of alginate–chitosan nanoparticle complexes. Transfection was determined by flow cytometry at 48 h, measuring (a) proportion of cells expressing GFP, and (b) change in mean fluorescence intensity. Transfection was evident only in 293T and COS7 cells using complexes prepared at a 5:1 N:P ratio. 293T cells are transfected with 6-fold greater efficiency than COS7 cells in terms of cell population (a), but with only twice the ΔMFI (b). Values represent the means ± standard deviation ($n = 3$). Stars represent significant difference from cells transfected with naked pDNA, with $P < 0.05$. LF, Lipofectamine™; pDNA, naked pEGFP-N1 plasmid.

Among the ratios tested, transfection was greatest with 293T cells using complexes prepared at an N:P ratio of 5:1, exhibiting greater transfection efficiency than Lipofectamine™ (not significantly different) though with comparably reduced protein production. Similarly, COS7 cells were transfected most efficiently with complexes prepared at a ratio of 5:1, showing 4-fold greater efficiency than naked DNA. However, transfection efficiency in this cell line remained significantly lower than was achieved with Lipofectamine™. In contrast, alginate–chitosan nanoparticle complexes did not mediate transfection in CHO cells, where the efficiency was on par with naked DNA.

3.3. Binding, internalization, and intracellular trafficking

3.3.1. Confocal microscopy analysis

Confocal microscopy was used to investigate complex uptake in each cell line and to examine subsequent internal trafficking. Cells were incubated with complexes prepared using fluorescein-labeled chitosan and treated with LysoTracker Red, a pH sensitive dye that fluoresces in the acidic environment of lysosomes, and with DAPI to label nuclei.

In 293T cells, complexes were observed bound to the cell membrane at 30 min (Fig. 3). The fluorescence appeared spotted on the cell surface rather than in a homogeneous covering, suggesting that the complexes were binding to distinct areas on the cell surface through specific interactions. This is further rationalized by the noted complex aggregation in some areas, as indicated by larger and brighter regions than would be expected from singular complexes. By 1 h post-treatment, complexes were visible as discrete points and in distinct compartments within the cells, suggesting that numerous complexes may have been entrapped within single endosomes. After 2 h, fluorescein fluorescence was no longer confined to distinct patches; diffuse, homogeneous, intracellular fluorescence was observable for the first time. At this time, fluorescence was evident in peri-nuclear locations and also co-localized with the nucleus. Diffuse fluorescence throughout the cell, including the nucleus, remained evident 4 h post-treatment.

Initial binding of complexes to COS7 cells occurred in a similar fashion to 293T cells, with distinct surface localization apparent 30 min following treatment. Some larger and brighter areas were also evident (Fig. 3). Internalized complexes were visible as early as 30 min, present as discrete points indicative of single complexes. Nuclear co-localization was also observable as early as 30 min post-treatment, suggesting that internalization and internal trafficking processes may be more rapid in this cell line. After 2 h, intracellular fluorescence began to appear in larger, brighter compartments, suggestive of vesicles containing numerous complexes. The size of these patches increased by 4 h post-treatment, with a corresponding decrease in the number of singular points. Fluorescence was never dispersed homogenously throughout the cell.

In CHO cells, membrane-bound complexes appeared predominantly as distinct spots 30 min post-treatment, though to a considerably reduced degree relative to COS7 and 293T cells (Fig. 3). After 1 h, fluorescence was visible in distinct compartments intracellularly that varied in size but were generally larger than single complexes, suggesting vesicular confinement of numerous complexes. As with COS7 cells, the number and size of these vesicles continued to grow through 4 h post-treatment with a coincident reduction in the number of singular complex points. By 4 h post-treatment, all fluorescence remained confined to distinct compartments, though the brightness and quantity had diminished. This may have resulted from trafficking leading to expulsion of the particles from the cells, or from dilution following cell division, as suggested by the altered cellular morphology.

In all three cell lines, binding of alginate–chitosan nanoparticle complexes occurred at distinct areas on the cell surface, with subsequent internalization and trafficking clearly differing between cell lines.

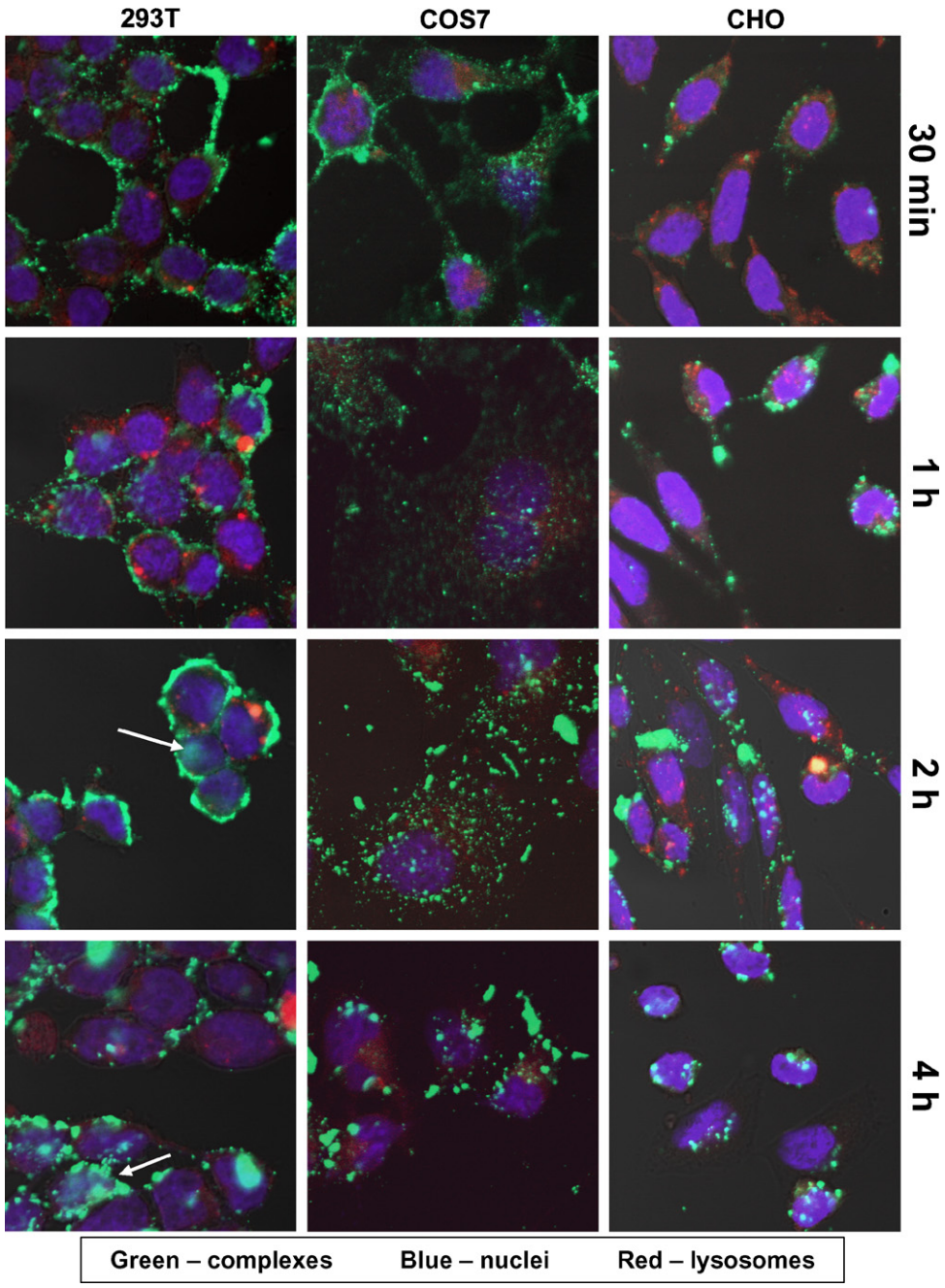

Fig. 3. Tracking fluorescein-labeled complex internalization in 293T, COS7, and CHO cells. Additional staining of nuclei (DAPI-blue) and lysosomes (LysoTracker Red). Thirty minutes post-treatment, complexes are bound to the cell membrane and have begun entering cells. The spotted appearance of complexes on membranes suggests a specific interaction with surface features. After 1 h, complexes were internalized; some were located in distinct compartments suggestive of vesicles. With time, the number and size of vesicle entrapped complexes increased in CHO and COS7 cells, as seen at 2 h and 4 h. By 4 h, complexes were co-localized with the nucleus in all cell lines, though in patches in CHO and COS7 cells. Diffuse homogenous fluorescence was only seen in 293T cells (arrows).

3.3.2. *Flow cytometry analysis*

Having qualitatively analyzed complex uptake in the various cell lines, flow cytometry was used to obtain more quantitative information regarding the interaction between complexes and cells. In all three cell lines binding and internalization of complexes was rapid and efficient (Fig. 4). The interaction between cells and complexes occurred almost immediately, with significant fluorescence detected within 15 min. Notably, COS7 cells exhibited an extremely rapid association with complexes; 57% demonstrated associated fluorescence following exposure of less than 1 min. The fraction of cells exhibiting fluorescence increased sharply over the first hour, reaching a plateau by 2 h post-treatment in all cell lines. At this time, the fractions of cells with bound or internalized complexes in 293T, COS7, and CHO cell lines were 79%, 91%, and 97%, respectively. The con-

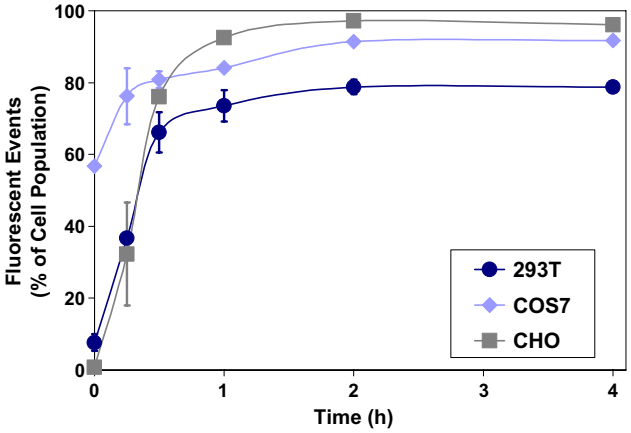

Fig. 4. Binding and internalization of fluorescein-labeled complexes. Note the immediate high association with COS7 cells. Values represent the means ± standard deviation of the fraction of the cell population showing fluorescence ($n \geqslant 3$).

siderable difference between 293T and CHO cell populations may in part be attributed to greater numbers of complexes binding to individual 293T cells as compared to CHO cells (Fig. 3), so that there were insufficient complexes to bind to all cells.

To measure fluorescence only from internalized complexes, cells were treated with trypan blue to quench external fluorescence prior to analysis. This produced similar curves for each cell line with a 30 min delay: a steep signal increase was apparent after 30 min, ultimately reaching the same plateau as without quenching. Thus, fluorescence measured at 2 h post-treatment with and without trypan blue quenching are equivalent, indicating that they are largely attributable to internalized rather than surface-bound complexes. It is evident that external binding occurs immediately with sufficient attraction to withstand washing, followed by the slower process of complex internalization. These results confirm that internalization of the complexes is efficient in each cell line, and is therefore not the cause of the discrepant transfection efficiencies.

3.4. Protein-mediated surface interactions

To further elucidate differences in the uptake mechanisms, the nature of complex interactions with cell membranes was investigated by treating cells with trypsin–EDTA prior to analysis to cleave surface proteins. Trypsinization resulted in decreased cell-associated fluorescence at 30 min, at which time fluorescence can be considered to be predominantly membrane-bound (Table 1). The 293T and COS7 cell lines demonstrated a substantial decrease (75–85%) in cell-associated fluorescence following trypsinization, indicating that complexes were attached to cells through trypsin-cleavable proteins. In contrast, CHO cells demonstrated a considerably smaller reduction (15%), signifying that the majority of complexes were not bound to the surface through trypsin-sensitive proteins.

Table 1
Involvement of surface proteins on binding (30 min) and uptake (2 h) of complexes in three cell lines

	293T (%)	COS7 (%)	CHO (%)
Trypsinization			
30 min	24 ± 3	15 ± 1	85 ± 4
Excess chitosan			
30 min	49 ± 7	40 ± 6	109 ± 3
2 h	50 ± 2	42 ± 1	89 ± 0

Results are expressed as the measured cell-associated fluorescence relative to untreated cells and are all statistically significant.
Values represent means ± standard deviation ($n = 3$).

To further investigate the involvement of surface proteins, the uptake assay was repeated in the presence of excess chitosan. Since the alginate–chitosan nanoparticle complexes display chitosan amino groups at the surface [13], this would reduce binding mediated by a specific ligand-receptor interaction. Unlabeled chitosan was added to the treatment medium in an amount equivalent to that present in the complexes. In 293T and COS7 cells, both binding and internalization were affected by excess chitosan, as indicated by decreased readings (50–60%) at 30 min and 2 h post-treatment (Table 1). These results support the hypothesis that specific interactions may be involved in cell binding of complexes. Conversely, cell-associated fluorescence of CHO populations was somewhat increased at 30 min (9%), and slightly decreased (11%) at 2 h. Given these findings, it is clear that cell membrane physiology affects the binding of alginate–chitosan nanoparticle complexes.

3.5. Intracellular trafficking to lysosomes

Although internalization was effective in each cell line, differences in uptake pathways could affect the intracellular fate of complexes, potentially contributing to the noted differences in transfection. Cells were assessed to evaluate the trafficking of complexes to lysosomes, where transfection could be prevented by degradation or digestion. Since fluorescein reversibly loses fluorescence below pH 5.5, transfer of complexes to lysosomes would quench fluorescence; co-incubation with an endosomolytic agent can prevent transfer to lysosomes and thus counter quenching. Thus, increased fluorescence resulting from treatment with an endosomolytic agent would suggest that complexes were being trafficked to lysosomes.

Treatment with chloroquine, which causes endosome rupture and content release to the cytosol, did not increase measured fluorescence in any of the cell lines, suggesting that complexes were not trapped in lysosomes (Fig. 5). For additional verification, a separate assay was conducted whereby cells were treated with monensin, which re-establishes neutral pH in lysosomes, following detachment and prior to analysis. Treatment with monensin failed to reveal any significant changes in cell-associated fluorescence, as

would be expected if complexes were trapped in an acidic environment. It can therefore be concluded that complexes are either not trafficked to or are able to escape from lysosomes in all three cell lines.

3.6. Mechanisms of nanoparticle–DNA complex endocytosis

The endocytic pathways used for complex internalization in each cell line were then investigated. Flow cytometry analysis of complex internalization was repeated under conditions known to affect specific endocytosis pathways. Treatment with chlorpromazine, an inhibitor of clathrin-dependent endocytosis, had significant effects on 293T and COS7 cell lines (Fig. 5). The reduction in internalization was greatest in 293T cells, where cell-associated fluorescence was reduced by 66%, as compared to the more moderate reduction in COS7 cells (33%) and no significant effect in CHO cells (10%). In contrast, genistein, an inhibitor of caveolin-dependent endocytosis, resulted in greater reductions in complex internalization in both COS7 (75%) and CHO (76%) cells, with a lesser effect in 293T cells (32%). Phorbol myristate acetate (PMA), a macropinocytosis stimulator, did not increase complex internalization in any cell line, and rather induced a slight decrease in CHO cells, indicating that macropinocytosis was not involved in complex uptake. In contrast, interruption of actin microfilament polymerization and depolymerization processes by cytochalasin D led to reduced internalization in 293T cells (60%) but had no significant effect on COS7 (5%) or CHO cells (7%). These data suggest that both clathrin- and caveolin-dependent routes were involved in the internalization of complexes in 293T and COS7 cells, while CHO cells exclusively used clathrin-independent routes. Furthermore, a separate mechanism involving actin microfilaments was active in 293T cells but not in the other cell lines.

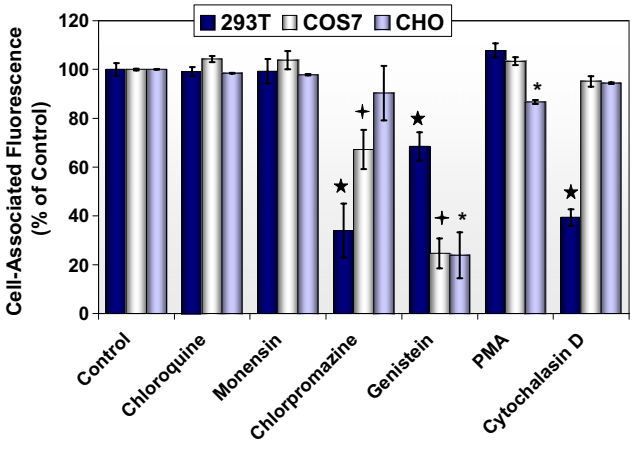

Fig. 5. Effects of inhibitors on internalization of fluorescein-labeled alginate–chitosan nanoparticle complexes. Monensin treatment was done prior to analysis, while chloroquine was applied with complexes. For the remaining treatments, cells were pre-treated 30 min prior to treatment with complexes. After 2 h, cells were analyzed by flow cytometry. Values indicate means ± standard deviations ($n = 3$). Stars indicate significant difference from the respective controls, with $P < 0.05$.

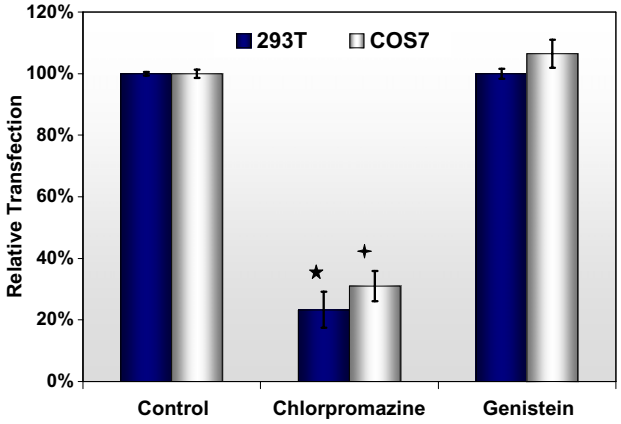

Fig. 6. Effects of endocytosis inhibitors on transfection. Transfection was performed with the luciferase plasmid. Cells were pre-treated with chlorpromazine or genistein for 30 min prior to treatment with alginate–chitosan nanoparticle–DNA complexes. Note that chlorpromazine treatment led to reduced transfection in 293T and COS7 cell lines, whereas genistein had no effect. The level of luciferase production (RLU/mg protein) in cells treated with complexes alone was set as 100%. Values indicate means ± standard deviations ($n = 3$). Stars indicate significant difference from controls ($P < 0.05$).

3.7. Effect of endocytosis inhibitors on transfection

The relationship between internalization pathways and transfection was investigated through transfection studies in the presence of the chemical inhibitors for the clathrin- and caveolin-mediated pathways (chlorpromazine and genistein, respectively). Treatment with chlorpromazine significantly reduced transfection in both 293T and COS7 cells (Fig. 6). In contrast, treatment with genistein had no effect on transfection in either cell line. This suggests that the clathrin-mediated pathway led to transfection with these complexes, whereas the caveolin-mediated pathway did not.

4. Discussion

Several studies have noted cell line-dependent transfection efficiency with a variety of non-viral vectors. The goal of the present work was to determine the cause of this cell line dependency by investigating the relationships between transfection and cellular binding and internalization mechanisms in three cell lines. Alginate–chitosan nanoparticle complexes, whose development we recently reported [13], were used to transfect 293T, COS7, and CHO cells, with results indicating strong cell line dependence. Transfection is considerably higher in 293T cells than COS7 cells, as measured by the percentage of cells expressing GFP, whereas there is virtually no transfection in CHO cells (Fig. 2); GFP production is also greater in 293T cells than COS7 cells, though the difference is more moderate. Condi-

tions leading to transfection with the complexes in both COS7 and 203T cell lines were also associated with a decrease in cell viability (Fig. 1). Interestingly, the equivalent transfection achieved in 293T cells treated with Lipofectamine™ or with complexes prepared at a 5:1 N:P ratio is achieved under conditions which are similarly cytotoxic. Though alginate–chitosan nanoparticle complexes are considerably less toxic than Lipofectamine™, these results support other studies reporting a relationship between transfection and observed cytotoxicity [20].

Flow cytometry and confocal microscopy studies confirm that the initial stage of transfection, complex binding and uptake, is a rapid and efficient process in all three cell lines, substantiating the notion that poor transfection results do not necessarily correlate with inadequate internalization of the complexes (Figs. 3 and 4) [3]. COS7 cells demonstrated a remarkable ability to bind complexes immediately upon exposure, with 57% of cells showing associated fluorescence following contact of less than 1 min. However, this rapid binding did not correlate with either increased internalization or transfection.

Confocal microscopy demonstrates that complexes bind to specific sites on cell membranes, as illustrated by the spotted patterns of fluorescence on the membranes (Fig. 3). Further supporting the hypothesis that surface-bound complexes are associated with membrane proteins is the considerably reduced binding upon treatment with trypsin, where a 75–85% decrease in cell-associated fluorescence occurred at 30 min in 293T and COS7 cells (Table 1). Moreover, supplementing the treatment medium with chitosan led to a considerable decrease in surface-bound complexes in the same cell lines, typical of competition assays for receptor-mediated endocytosis, further suggesting the involvement of specific interactions in complex binding. In contrast, neither trypsinization nor the presence of chitosan had a substantial effect on the measured binding of complexes to CHO cells. Complex binding to these cells may not involve proteins, or may involve membrane features that are insensitive to trypsin. Since confocal microscopy revealed non-homogeneous membrane binding in this cell line, the latter case is considered more likely (Fig. 3).

The decreased binding of complexes in the presence of excess chitosan could also be indicative that the complexes interact through non-specific charge interactions with molecules on the cell surface. However, non-specific charge interactions have been attributed to the same membrane components involved in Ca^{2+}-mediated anchoring of the cell and cell-surface heparin sulphate proteoglycans (HSPGs) [21–24]. Although the involvement of HSPGs, which are only significantly expressed in non-confluent cells, has been used to explain the increased transfection observed in dividing cells, it does not explain the differences in binding observed in this study, since all three cell lines are known to express HSPGs. Alternatively, a recent study suggests that the mannose receptor may be involved in oligochitosan binding and uptake in macrophages [25]. The results of this study endorse the involvement of this receptor, given that 293T and COS7 cells express the mannose receptor, and that CHO cells, which do not express this receptor, were unaffected by trypsinization and excess chitosan [26]. Clearly, cell membrane physiology is a determining factor in complex binding.

Given that binding and internalization is successful in each cell line, chemical inhibitors of specific endocytic processes were employed to determine if discrete pathways lead to transfection. Results of uptake assays under inhibition in 293T cells indicate that clathrin-dependent endocytosis plays a significant role in complex internalization, with a 66% reduction observed under chlorpromazine treatment. Actin microfilaments also contribute significantly, as demonstrated by a 60% reduction with cytochalasin D treatment. Caveolin inhibition with genistein had a considerably smaller impact on internalization in 293T cells (33% reduction). In COS7 cells, clathrin inhibition had a comparatively reduced impact (33% reduction), while caveolin inhibition induced a substantial reduction in internalization (75%). Treatment with cytochalasin D did not reduce uptake significantly (5%), indicating that internalization via actin-mediated pathways is not significant in COS7 cells. Finally, CHO cells demonstrate a strong dependence on caveolin for internalization of complexes, with a 76% reduction observed with genistein treatment. While no effects were observed with inhibition of clathrin or actin microfilaments, it is evident that other internalization pathway(s) are involved since obstruction of caveolin-mediated pathways did not completely eliminate complex uptake. Though the reasons for cell line dependence remain unconfirmed, these results support the suggestion that the mechanism of complex internalization is affected by cell membrane composition and physiology [16,27].

Since all three cell lines express both clathrin and caveolin proteins, the reasons for alternative uptake pathways are not immediately evident. It has previously been reported that complex size can affect the mechanism of internalization, with clathrin-mediated processes limited to particles under 200 nm, and caveolin-dependent uptake prevailing for particles between 200 and 500 nm [7]. However, pathway dependencies observed in this study cannot be explained by size since all cells were treated with the same preparations of complexes. Nor can these results be explained by the composition of the complexes [4], since the same complexes were clearly shown to be internalized via different pathways. Rather, these findings support other studies that collectively infer that cell physiology is critical in complex internalization [28–30]. The combined effects of complex size, composition, and cell physiology on internalization pathways require additional investigation as knowledge of these interactions is essential for designing effective transfection vectors.

The disparate endocytic pathways of the complexes attain increased significance upon consideration of the relationship between internalization mechanism and transfection efficiency. Transfection studies performed with

luciferase plasmid in the presence of inhibitors of clathrin- or caveolin-mediated endocytosis confirm the importance of specific internalization mechanisms for successful transfection. In 293T cells, transfection was inhibited by the clathrin inhibitor but not by the caveolin inhibitor, in accordance with the internalization studies (Figs. 5 and 6). Surprisingly, similar results were obtained with transfection of COS7 cells, though they showed a greater dependence on caveolin-mediated endocytosis. These results suggest that clathrin-mediated internalization is required for efficient transfection using alginate–chitosan nanoparticle complexes.

Since complex internalization is effective in all cells regardless of the pathway, the observed cell line-dependent transfection must be determined by the fate of complexes post-internalization. Transfer of internalized material to lysosomes, where it is degraded by the acidic environment and various enzymes, is believed to be the greatest barrier to effective transfection [4]. However, internalization assays with chloroquine or monensin treatment did not change measured fluorescence in any cell line, indicating that complexes are not entrapped in highly acidic environments (Fig. 5). Moreover, confocal microscopy failed to show significant co-localization of complexes with LysoTracker Red (Fig. 3), suggesting that acidic or enzymatic degradation in lysosomes is not a reasonable explanation for the observed internalization pathway-dependent transfection discrepancies.

Pathways leading to efficient transfection, and the requisite subsequent internal trafficking, can be intimated from investigation of the confocal microscopy images. Fluorescence in COS7 and CHO cells occurs in distinct patches that grow in size and number following internalization. The manifestation of fluorescence in distinct compartments in CHO and COS7 cells suggests that complexes remain trapped within vesicles. In contrast, the homogeneous, diffuse fluorescence observed in 293T cells after 2 h indicates that complexes escape from vesicles, ultimately leading to transfection [31]. A recent study reports similar findings: PEI complexes that escape endosomes in 293T cells are transfection competent, whereas PLL complexes that remain entrapped in vesicles do not mediate transfection [32]. Thus, the ability to escape vesicles, which is affected by the internalization mechanism, is a critical barrier to efficient transfection.

Several hypotheses have been proposed to explain the escape of complexes from endosomes. It has been suggested that chitosan nanoparticles are able to escape the endo-lysosomal pathway through the proton-sponge effect, due to their abundance of amine groups [33]. The sequestration of protons during acidification of secondary endosomes leads to segregation between the protons and their counter-ions, resulting in increased osmotic pressure, osmotic swelling, and ultimate rupture of the vesicles [34]. The complexes used in this study, composed of alginate and an excess of chitosan, are capable of mediating this effect. However, the results of this study suggest that the mechanism of endosomal escape is dependent on the internalization mechanism, and thus cell line. While the proton-sponge mechanism also explains the lack of complex co-localization with and trafficking to lysosomes, its failure to mediate vesicle escape in CHO and COS7 cells requires an alternate explanation.

Studies with polyplexes in A549 and HeLa cells have shown that clathrin-mediated endocytosis leads to trafficking to the endo-lysosomal pathway, whereas the caveolin-mediated pathway does not, due to the absence in caveosomes of signaling molecules required for interaction with other cellular compartments [4]. This avoidance of transfer to the endo-lysosomal pathway can explain the entrapment of complexes in vesicles in CHO and COS7 cells, as has been observed with PLL-based vectors in HepG2 cells [35].

Based on the results of this study, the following binding and internalization mechanisms of the complexes in each cell line are proposed (Fig. 7):

(1) In 293T cells, complexes bind to the surface by means of specific interactions and are subsequently internalized through a variety of endocytic pathways, dominated by clathrin- and microfilament-mediated processes. Following internalization, complexes are trafficked to late endosomes and/or lysosomes, where acidification is countered by the proton-sponge pH buffering capacity of chitosan within the complexes. This effect results in endosomal rupture, escape of the complexes, and ultimately leads to transfection.

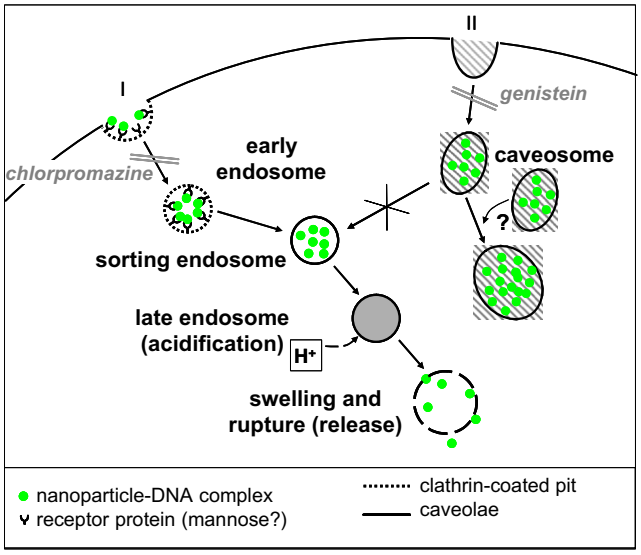

Fig. 7. Proposed uptake pathways and intracellular trafficking of alginate–chitosan nanoparticle–DNA complexes. (I) In 293T and COS7 cells, complexes are internalized via clathrin-dependent endocytosis following protein-mediated binding, where they are transferred to sorting endosomes. Complexes are transferred to late endosomes where acidification begins, leading to rupture and release due to the proton-sponge effect. (II) In CHO and COS7 cells, complexes are internalized through caveolin-dependent endocytosis. Following uptake, complexes remain trapped in caveosomes, which lack signal molecules for trafficking, where they become transfection incompetent. Caveosomes may fuse leading to large vesicles of entrapped complexes.

(2) While complexes also bind to COS7 cells through interactions with specific surface features, they are predominantly internalized via caveolin-mediated endocytosis. Complexes entering through the clathrin-dependent process are presumed to be trafficked similarly as in 293T cells, leading to transfection. In contrast, complexes internalized by caveolin-mediated endocytosis are entrapped in caveosomes but are not trafficked to the endo-lysosomal pathway. Since these vesicles do not undergo acidification, there remains no mechanism for the complexes to escape; they consequently remain entrapped in vesicles where they cannot mediate transfection.

(3) Trypsin and competition binding assays indicate no evidence for the involvement of proteins in complex binding to CHO cells. Inhibition assays demonstrate that the internalization mechanism of complexes is primarily through caveolin-mediated endocytosis. As with COS7 cells, this pathway was transfection incompetent, resulting in the entrapment of complexes within vesicles.

Although it remains unclear why the internalization mechanisms of the complexes differed between cell lines, successful transfection is evidently dependent on the internalization pathway as it relates to their intracellular trafficking. For these complexes, transfection requires trafficking to the endo-lysosomal pathway, where the proton-sponge effect allows them to escape and mediate transfection. In these cell lines, this seems to occur via clathrin-dependent endocytosis, but not through caveolin-dependent endocytosis. The inclusion of design elements to direct these complexes to late endosomes of the clathrin-dependent endocytic pathway could further improve their transfection efficiency in multiple cell lines.

5. Conclusions

The results of this study suggest that cell line-dependent transfection efficiency is related to internalization mechanisms and subsequent internal trafficking of the vectors. Alginate–chitosan nanoparticle complexes were shown to mediate transfection in 293T and COS7 cells, but did not lead to transfection in CHO cells. Internalization studies indicate that effective transfection follows clathrin-mediated endocytosis of the complexes. Clathrin-dependent endocytosis accounted for the majority of internalized complexes in 293T cells, and a fraction of those that penetrated COS7 cells. Conversely, complexes were found to enter CHO cells predominantly through caveolin-dependent endocytosis, which did not lead to transfection. Transfection studies in the presence of inhibitors confirm these pathway dependencies.

Transfection efficiency was found to be affected by the internalization pathway as it relates to intracellular trafficking. Complexes that entered cells through transfection-competent pathways were trafficked to the endo-lysosomal pathway where they were able to escape, presumably due to the proton-sponge effect. Complexes were then able to enter the nucleus and mediate transfection. In contrast, complexes that entered cells through caveolin-mediated processes were not trafficked to the endo-lysosomal pathway and thus were unable to escape from the vesicles, remaining trapped and ineffective for transfection.

This study demonstrates that different internalization mechanisms lead to disparate transfection efficiencies in diverse cell lines. While both the composition and size of complexes have been proposed as influencing internalization mechanisms, this study clearly indicates that cell physiology is also a dominant factor, since the same complexes were internalized and trafficked differently in three cell lines. Although the reasons for the different uptake mechanisms remain unclear, this study underscores the importance of understanding the cellular interaction and internalization mechanisms of non-viral vectors. Knowledge of these mechanisms is critical for the development of efficient vectors that can exploit transfection-effective pathways in diverse cell lines through designs that favor endosomal escape and delivery to the cytoplasm and nucleus.

Acknowledgements

The authors thank Shawn Carrigan for expert assistance with manuscript preparation. We would like to acknowledge the Natural Sciences and Engineering Research Council of Canada (NSERC), the Fonds québécois de la recherche sur la nature et les technologies (FQRNT), and the Canadian Institutes of Health Research (CIHR) for funding this research.

References

[1] S. Danielsen, K.M. Varum, B.T. Stokke, Structural analysis of chitosan mediated DNA condensation by AFM: influence of chitosan molecular parameters, Biomacromolecules 5 (2004) 928–936.
[2] S. Hirosue, B.G. Muller, R.C. Mulligan, R. Langer, Plasmid DNA encapsulation and release from solvent diffusion nanospheres, J. Control Release 70 (2001) 231–242.
[3] A. Akinc, D.G. Anderson, D.M. Lynn, R. Langer, Synthesis of poly(beta-amino ester)s optimized for highly effective gene delivery, Bioconjug. Chem. 14 (2003) 979–988.
[4] J. Rejman, A. Bragonzi, M. Conese, Role of clathrin- and caveolae-mediated endocytosis in gene transfer mediated by lipo- and polyplexes, Mol. Ther. 12 (2005) 468–474.
[5] M. Huang, Z. Ma, E. Khor, L.Y. Lim, Uptake of FITC–chitosan nanoparticles by A549 cells, Pharm. Res. 19 (2002) 1488–1494.
[6] M. Manunta, P.H. Tan, P. Sagoo, K. Kashefi, A.J. George, Gene delivery by dendrimers operates via a cholesterol dependent pathway, Nucl. Acids Res. 32 (2004) 2730–2739.
[7] J. Rejman, V. Oberle, I.S. Zuhorn, D. Hoekstra, Size-dependent internalization of particles via the pathways of clathrin- and caveolae-mediated endocytosis, Biochem. J. 377 (2004) 159–169.
[8] S. Prabha, W.Z. Zhou, J. Panyam, V. Labhasetwar, Size-dependency of nanoparticle-mediated gene transfection: studies with fractionated nanoparticles, Int. J. Pharm. 244 (2002) 105–115.
[9] W.T. Godbey, A.G. Mikos, Recent progress in gene delivery using non-viral transfer complexes, J. Control Release 72 (2001) 115–125.
[10] H. Akita, R. Ito, I.A. Khalil, S. Futaki, H. Harashima, Quantitative three-dimensional analysis of the intracellular trafficking of plasmid

DNA transfected by a nonviral gene delivery system using confocal laser scanning microscopy, Mol. Ther. 9 (2004) 443–451.
[11] N. Laurent, C.S. Wattiaux-De, E. Mihaylova, E. Leontieva, M.T. Warnier-Pirotte, R. Wattiaux, M. Jadot, Uptake by rat liver and intracellular fate of plasmid DNA complexed with poly-L-lysine or poly-D-lysine, FEBS Lett. 443 (1999) 61–65.
[12] M. Huang, E. Khor, L.Y. Lim, Uptake and cytotoxicity of chitosan molecules and nanoparticles: effects of molecular weight and degree of deacetylation, Pharm. Res. 21 (2004) 344–353.
[13] K.L. Douglas, C. Piccirillo, M. Tabrizian, Effects of alginate inclusion on the vector properties of chitosan-based nanoparticles, Controlled Release Systems 115 (2006) 354–361.
[14] H.Q. Mao, K. Roy, L. Troung, K.A. Janes, K.Y. Lin, Y. Wang, J.T. August, K.W. Leong, Chitosan–DNA nanoparticles as gene carriers: synthesis, characterization and transfection efficiency, J. Control Release 70 (2001) 399–421.
[15] J. Akbuga, S. Ozbas-Turan, N. Erdogan, Plasmid-DNA loaded chitosan microspheres for in vitro IL-2 expression, Eur. J. Pharm. Biopharm. 58 (2004) 501–507.
[16] T. Dastan, K. Turan, In vitro characterization and delivery of chitosan–DNA microparticles into mammalian cells, J. Pharm. Pharm. Sci. 7 (2004) 205–214.
[17] S. Werth, B. Urban-Klein, L. Dai, S. Hobel, M. Grzelinski, U. Bakowsky, F. Czubayko, A. Aigner, A low molecular weight fraction of polyethylenimine (PEI) displays increased transfection efficiency of DNA and siRNA in fresh or lyophilized complexes, J. Control Release 112 (2006) 257–270.
[18] L.B. Jacobsen, S.A. Calvin, K.E. Colvin, M. Wright, FuGENE 6 transfection reagent: the gentle power, Methods 33 (2004) 104–112.
[19] K.M. Tyner, M.S. Roberson, K.A. Berghorn, L. Li, R.F. Gilmour Jr., C.A. Batt, E.P. Giannelis, Intercalation, delivery, and expression of the gene encoding green fluorescence protein utilizing nanobiohybrids, J. Control Release 100 (2004) 399–409.
[20] K. Corsi, F. Chellat, L'H. Yahia, J.C. Fernandes, Mesenchymal stem cells, MG63 and HEK 293 transfection using chitosan–DNA nanoparticles, Biomaterials 24 (2003) 1255–1264.
[21] W.T. Godbey, K.K. Wu, A.G. Mikos, Tracking the intracellular path of poly(ethylenimine)/DNA complexes for gene delivery, Proc. Natl. Acad. Sci. USA 96 (1999) 5177–5181.
[22] W.T. Godbey, K.K. Wu, A.G. Mikos, Poly(ethylenimine) and its role in gene delivery, J. Control Release 60 (1999) 149–160.
[23] I. Kopatz, J.S. Remy, J.P. Behr, A model for non-viral gene delivery: through syndecan adhesion molecules and powered by actin, J. Gene. Med. 6 (2004) 769–776.
[24] M. Feng, D. Lee, P. Li, Intracellular uptake and release of poly(ethyleneimine)-co-poly(methyl methacrylate) nanoparticle/pDNA complexes for gene delivery, Int. J. Pharm. 311 (2006) 209–214.
[25] Y. Han, L. Zhao, Z. Yu, J. Feng, Q. Yu, Role of mannose receptor in oligochitosan-mediated stimulation of macrophage function, Int. Immunopharmacol. 5 (2005) 1533–1542.
[26] Y. Su, T. Bakker, J. Harris, C. Tsang, G.D. Brown, M.R. Wormald, S. Gordon, R.A. Dwek, P.M. Rudd, L. Martinez-Pomares, Glycosylation influences the lectin activities of the macrophage mannose receptor, J. Biol. Chem. 280 (2005) 32811–32820.
[27] R. Cartier, R. Reszka, Utilization of synthetic peptides containing nuclear localization signals for nonviral gene transfer systems, Gene Ther. 9 (2002) 157–167.
[28] Y. Mo, L.Y. Lim, Mechanistic study of the uptake of wheat germ agglutinin-conjugated PLGA nanoparticles by A549 cells, J. Pharm. Sci. 93 (2004) 20–28.
[29] J. Panyam, W.Z. Zhou, S. Prabha, S.K. Sahoo, V. Labhasetwar, Rapid endo-lysosomal escape of poly(DL-lactide-co-glycolide) nanoparticles: implications for drug and gene delivery, FASEB J. 16 (2002) 1217–1226.
[30] M.G. Qaddoumi, H.J. Gukasyan, J. Davda, V. Labhasetwar, K.J. Kim, V.H. Lee, Clathrin and caveolin-1 expression in primary pigmented rabbit conjunctival epithelial cells: role in PLGA nanoparticle endocytosis, Mol. Vis. 9 (2003) 559–568.
[31] M. Ogris, R.C. Carlisle, T. Bettinger, L.W. Seymour, Melittin enables efficient vesicular escape and enhanced nuclear access of nonviral gene delivery vectors, J. Biol. Chem. 276 (2001) 47550–47555.
[32] K. Itaka, A. Harada, Y. Yamasaki, K. Nakamura, H. Kawaguchi, K. Kataoka, In situ single cell observation by fluorescence resonance energy transfer reveals fast intra-cytoplasmic delivery and easy release of plasmid DNA complexed with linear polyethylenimine, J. Gene. Med. 6 (2004) 76–84.
[33] M. Koping-Hoggard, K.M. Varum, M. Issa, S. Danielsen, B.E. Christensen, B.T. Stokke, P. Artursson, Improved chitosan-mediated gene delivery based on easily dissociated chitosan polyplexes of highly defined chitosan oligomers, Gene Ther. 11 (2004) 1441–1452.
[34] H. Kamiya, H. Tsuchiya, J. Yamazaki, H. Harashima, Intracellular trafficking and transgene expression of viral and non-viral gene vectors, Adv. Drug Deliv. Rev. 52 (2001) 153–164.
[35] C. Goncalves, E. Mennesson, R. Fuchs, J.P. Gorvel, P. Midoux, C. Pichon, Macropinocytosis of polyplexes and recycling of plasmid via the clathrin-dependent pathway impair the transfection efficiency of human hepatocarcinoma cells, Mol. Ther. 10 (2004) 373–385.